

Mathematical Adjoint Solution to Analytic Function Expansion Nodal (AFEN) Method

Nam Zin Cho and Ser Gi Hong

Korea Advanced Institute of Science and Technology

(Received January 28, 1995)

해석함수전개 노달방법의 수학적 수반해

조남진 · 홍서기

한국과학기술원

(1995. 1. 28 접수)

Abstract

The mathematical adjoint solution of the Analytic Function Expansion (AFEN) method is found by solving the transposed matrix equation of AFEN nodal equation with only minor modification to the forward solution code AFEN. The perturbation calculations are then performed to estimate the change of reactivity by using the mathematical adjoint. The adjoint calculational scheme in this study does not require the knowledge of the physical adjoint or the eigenvalue of the forward equation. Using the adjoint solutions, the exact and first-order perturbation calculations are performed for the well-known benchmark problems (i.e., IAEA-2D benchmark problem and EPRI-9R benchmark problem). The results show that the mathematical adjoint flux calculated in the code is the correct adjoint solution of the AFEN method.

요 약

해석함수 전개 노달방법의 수학적 수반해를 AFEN코드에 약간의 수정을 통하여 AFEN노달 방정식의 전치행렬 방정식을 풀어서 계산 하였다. 또한 이 수반해를 사용하여 섭동이론(정확한 섭동이론과 일차근사 섭동이론)을 이용한 계산이 반응도 변화를 예측하기위해 두개의 잘 알려진 표준문제를 통하여 수행되었다. 본 연구에서 수반해의 계산방법은 물리적 수반해 및 정방정식의 고유치를 필요로 하지 않는다. 계산결과들은 본 논문에서 계산된 수반해가 AFEN방법의 정확한 수학적 수반해임을 보여준다.

1. Introduction

The adjoint solution is widely used for estimating the effects of changes in reactor systems for a range of reactor characteristics such as reaction ratios and fuel burnup. As nodal methods become powerful for

reactor core analysis, the need for the corresponding perturbation methods becomes evident. For reactor analysis, perturbation methods require the accurate solutions of the forward as well as the adjoint equations.

The usual perturbation formula that results, how-

ever, involves dot products of gradients of the forward and adjoint fluxes, and finding such gradients leads to a great error. To avoid this difficulty, the perturbation theory is derived from the matrix equation that is obtained from the nodal formulation of diffusion problem rather than from the differential equations from which the nodal formulation has been derived. The resultant perturbation theory requires so-called "the mathematical adjoint" that is obtained from transposing the nodal formula and then solving the transposed formula. On the other hand, the perturbation theory that is derived from the differential equation requires so-called "the physical adjoint" that can be obtained by reordering the input cross sections without significant modification of the nodal program, but it is not consistent with the perturbation theory of the nodal formulation.

The two adjoints are generally different from each other because of the asymmetry of the nodal formulation of the diffusion operator, whereas they are the same in the finite difference diffusion operator because of the symmetry of the finite difference diffusion operator. [1] Since the perturbation theory requires the mathematical adjoint to eliminate the first order error, the mathematical adjoint must be found. But it was believed that a considerable modification of the forward solution scheme needs to be made for the calculation of the mathematical adjoint. In particular, when the nodal equivalence theory is used, the neutron fluxes are allowed to be discontinuous at the nodal interfaces and the discontinuity factors are used to relate the heterogeneous and homogeneous fluxes. Lawrence[2] discovered that, in certain situations (that is, in the case of flat transverse leakage approximation), the mathematical adjoint is obtained by a similarity transformation of the physical adjoint which is, in turn, easy to calculate. However, this transformation method has fundamental problems. First, it is dependent on the transverse leakage term, which is only approximate and problematic, particularly in non-rectangular geometries. Secondly, the physical

adjoint is not well defined or cumbersome, if not impossible, to calculate in the presence of discontinuity factors that are the very corner-stone of the modern nodal methods.

Several attempts have been made to use perturbation theory for modern nodal methods to obtain reactivity changes. Taiwo[3] calculated the mathematical adjoint of the QUANDRY code by directly solving the transposed matrix equation of the QUANDRY formulation (direct solution scheme). But the forward equation was solved first to find the eigenvalue before the adjoint equation. Yang, Taiwo, and Khalil[4, 5] calculated the mathematical adjoint of an interface current nodal formulation both by a similarity transformation of the physical adjoint for flat transverse leakage approximation and by a direct solution scheme for both flat and quadratic transverse leakage approximations.

The objective of this paper is to show that it is possible and quite easy to calculate the mathematical adjoint in the AFEN formulation[6] (no transverse integration) by a direct solution scheme. Unlike Taiwo, the forward equation is not necessarily required to be solved before the adjoint equation. The transposed matrix equation is solved by the same scheme as in the forward solution. The physical adjoint is also obtained for only comparison purposes with the mathematical adjoint. The reactivity changes are estimated and computed by the exact and first-order perturbation methods to verify the mathematical adjoint calculated in the AFEN method.

2. Review of AFEN Method

In this section, the AFEN (Analytic Function Expansion Nodal) method is briefly reviewed to facilitate later presentation. This method directly solves the multidimensional diffusion equation instead of the transverse-integrated one-dimensional diffusion equations. It is accomplished by expanding the solution in terms of nonseparable analytic basis functions satisfying the diffusion equation at any point of the node. This ex-

pansion consists of eight basis functions and one additional constant term per node per group (for rectangular nodes). The nine coefficients are expressed in terms of nine nodal variables per node per group (i.e., one node-average flux, four node-interface fluxes, and four corner point fluxes). These nodal unknowns are then obtained by solving the nodal balance equations, current continuity equations, and corner-point equations. It is reported in several papers[6-10] that the above aspects of the AFEN method give highly accurate solutions even in the vicinity of the interface and corner point between assemblies having quite strong heterogeneity.

The two-group two-dimensional static diffusion equations for a homogenized square node n with node side h can be written as follows:

$$-D^n \nabla^2 \hat{\phi}^n(x, y) + \Sigma^n \hat{\phi}^n(x, y) = \frac{1}{k_{eff}} \nu \Sigma_f^n \hat{\phi}^n(x, y). \quad (1)$$

This equation is rewritten in more compact form as follows:

$$-\nabla^2 \hat{\phi}^n(x, y) + (D^n)^{-1} [\Sigma^n - \frac{1}{k_{eff}} \nu \Sigma_f^n] \hat{\phi}^n(x, y) = 0. \quad (2)$$

If λ_g^n are defined as the eigenvalues of the matrix $(D^n)^{-1} [\Sigma^n - \frac{1}{k_{eff}} \nu \Sigma_f^n]$ and matrix R^n as the 2×2 matrix with corresponding eigenvectors, and if a new unknown ξ defined by the relation

$$\hat{\xi}^n(x, y) = (R^n)^{-1} \hat{\phi}^n(x, y), \quad (3)$$

Eq.(2) is decoupled as follows:

$$\nabla^2 \hat{\xi}_g^n(x, y) - \lambda_g^n \hat{\xi}_g^n(x, y) = 0, \quad g = 1, 2. \quad (4)$$

Then, the general solution of Eq.(4) is expanded in terms of nine basis functions (of which each term satisfies Eq.(4) exactly) as follows:

$$\begin{aligned} \hat{\xi}_g^n(x, y) = & C_g^n + A_{g1}^n SN x_g^n x + A_{g2}^n CS x_g^n x + A_{g3}^n SN x_g^n y + A_{g4}^n CS x_g^n y + B_{g1}^n SN \frac{\sqrt{2}}{2} x_g^n x SN \frac{\sqrt{2}}{2} x_g^n y \\ & + B_{g2}^n SN \frac{\sqrt{2}}{2} x_g^n x CS \frac{\sqrt{2}}{2} x_g^n y + B_{g3}^n CS \frac{\sqrt{2}}{2} x_g^n x SN \frac{\sqrt{2}}{2} x_g^n y \\ & + B_{g4}^n CS \frac{\sqrt{2}}{2} x_g^n x CS \frac{\sqrt{2}}{2} x_g^n y, \end{aligned} \quad (5)$$

where

$$\begin{aligned} x_g^n &= (|\lambda_g^n|)^{1/2} \\ SN x_g^n u &= \begin{cases} \sinh x_g^n u, & \lambda_g^n > 0 \\ \sin x_g^n u, & \lambda_g^n < 0 \end{cases} \\ CS x_g^n u &= \begin{cases} \cosh x_g^n u, & \lambda_g^n > 0 \\ \cos x_g^n u, & \lambda_g^n < 0 \end{cases} \\ u &= x, y. \end{aligned} \quad (6)$$

The nine expansion coefficients can be expressed in terms of nine nodal unknowns but the details are omitted here (Ref. 6). The first nodal coupling equation imposed on the nodal unknowns is a nodal balance equation that is obtained by integrating Eq.(1) over the node volume:

$$\frac{1}{h} [(\bar{J}_{i+1j}^x - \bar{J}_{ij}^x) + (\bar{J}_{ij+1}^y - \bar{J}_{ij}^y)] + \Sigma_{ij}^0 \bar{\phi}_{ij} = \frac{1}{k_{eff}} \nu \Sigma_f^0 \bar{\phi}_{ij}. \quad (7)$$

The surface average currents in Eq. (7) can be expressed in terms of other nodal unknowns (i.e., interface fluxes $\tilde{\phi}$, node average flux $\bar{\phi}$, and corner point fluxes ϕ) and Eq.(7) is rewritten as follows:

$$\begin{aligned} & [\frac{8}{h} \langle a^0 w^0 \rangle + (D^0)^{-1} \Sigma^0] \bar{\phi}_{ij} = \\ & \frac{2}{h} \langle a^0 w^0 \rangle (F^0)^{-1} (\tilde{\phi}_{i+1j}^x + \tilde{\phi}_{ij+1}^x + \tilde{\phi}_{ij+1}^y + \tilde{\phi}_{ij}^y) \\ & + \frac{2}{h} \langle b^0 v^0 \rangle (F^0)^{-1} [(\phi_{ij} + \phi_{i+1j} + \phi_{ij+1} + \phi_{i+1j+1}) - (\tilde{\phi}_{i+1j}^x + \tilde{\phi}_{ij}^x + \tilde{\phi}_{ij+1}^y + \tilde{\phi}_{ij}^y)] \\ & + \frac{1}{k_{eff}} (D^0)^{-1} \nu \Sigma_f^0 \bar{\phi}_{ij}. \end{aligned} \quad (8)$$

where F^{ij} is the diagonal matrix whose elements are the discontinuity factors of the node, and a^0 , b^0 , w^0 and v^0 are diagonal matrices with elements also given in Ref. 6.

The symbol $\langle \cdot \rangle$ on a matrix denotes similarity transformation as

$$\langle \cdot \rangle = R^n \cdot (R^n)^{-1}. \quad (9)$$

The second nodal coupling equation is an interface current continuity equation that is derived by applying the continuity condition of the neutron currents across each node interface:

$$\begin{aligned} \mathbf{J}_{ij}^* &\equiv \mathbf{J}_{\text{at left surface of } ij \text{ th node}}^* \\ &= \mathbf{J}_{\text{at right surface of } i-1j \text{ th node}}^* \end{aligned} \quad (10)$$

Since the currents can be expressed in terms of the node average fluxes, interface fluxes, and corner point fluxes, this equation leads to the following block tridiagonal matrix equation:

$$T_{ij}^{\alpha, L} \bar{\phi}_{i-1j}^x + T_{ij}^{\alpha, C} \bar{\phi}_{ij}^x + T_{ij}^{\alpha, R} \bar{\phi}_{i+1j}^x = \mathbf{p}_{ij}^x, \quad (11)$$

where

$$\begin{aligned} T_{ij}^{\alpha, L} &= -D^{i-1j} \langle \mathbf{a}^{i-1j} (I - \mathbf{w}^{i-1j}) \rangle (F^{i-1j})^{-1} \\ T_{ij}^{\alpha, C} &= D^{i-1j} \langle \mathbf{a}^{i-1j} (I + \mathbf{w}^{i-1j}) \rangle (F^{i-1j})^{-1} \\ &\quad + D^{ij} \langle \mathbf{a}^{ij} (I + \mathbf{w}^{ij}) \rangle (F^{ij})^{-1} \\ T_{ij}^{\alpha, R} &= -D^{ij} \langle \mathbf{a}^{ij} (I - \mathbf{w}^{ij}) \rangle (F^{ij})^{-1}, \end{aligned} \quad (12)$$

and

$$\begin{aligned} \mathbf{p}_{ij}^x &= D^{i-1j} \langle \mathbf{b}^{i-1j} (I - \mathbf{v}^{i-1j}) \rangle \\ &\quad (F^{i-1j})^{-1} \frac{1}{2} (\phi_{i-1j+1} + \phi_{i-1j}) \\ &\quad - [D^{i-1j} \langle \mathbf{b}^{i-1j} (I + \mathbf{v}^{i-1j}) \rangle (F^{i-1j})^{-1} \\ &\quad + D^{ij} \langle \mathbf{b}^{ij} (I + \mathbf{v}^{ij}) \rangle (F^{ij})^{-1}] \frac{1}{2} (\phi_{ij+1} + \phi_{ij}) \\ &\quad + D^{ij} \langle \mathbf{b}^{ij} (I - \mathbf{v}^{ij}) \rangle (F^{ij})^{-1} \frac{1}{2} (\phi_{i+1j+1} + \phi_{i+1j}) \\ &\quad + 2D^{i-1j} \langle \mathbf{a}^{i-1j} \mathbf{w}^{i-1j} \rangle \bar{\phi}_{i-1j} + 2D^{ij} \langle \mathbf{a}^{ij} \mathbf{w}^{ij} \rangle \bar{\phi}_{ij} \\ &\quad + D^{i-1j} \langle \mathbf{b}^{i-1j} \mathbf{v}^{i-1j} \rangle (F^{i-1j})^{-1} (\bar{\phi}_{i-1j+1}^y + \bar{\phi}_{i-1j}^y) \\ &\quad + D^{ij} \langle \mathbf{b}^{ij} \mathbf{v}^{ij} \rangle (F^{ij})^{-1} (\bar{\phi}_{ij+1}^y + \bar{\phi}_{ij}^y). \end{aligned} \quad (13)$$

Finally, the corner point balance equation is derived on the basis of the neutron balance within a small box around the corner point that is shared by four adjacent nodes. The equation is given as follows:

$$\begin{aligned} T_{ij}^C \phi_{ij} + T_{ij}^L \phi_{i-1j} + T_{ij}^R \phi_{i+1j} \\ + T_{ij}^B \phi_{ij-1} + T_{ij}^T \phi_{ij+1} = q_{ij}, \end{aligned} \quad (14)$$

where

$$\begin{aligned} T_{ij}^C &= \sum_{u,v=0}^1 D^{i-uj-v} \langle \mathbf{c}^{i-uj-v} \rangle (F^{i-uj-v})^{-1} \\ T_{ij}^L &= \sum_{v=0}^1 \frac{1}{2} D^{i-1j-v} \langle \mathbf{c}^{i-1j-v} \rangle (F^{i-1j-v})^{-1} \\ T_{ij}^R &= \sum_{v=0}^1 \frac{1}{2} D^{ij-v} \langle \mathbf{c}^{ij-v} \rangle (F^{ij-v})^{-1} \\ T_{ij}^B &= \sum_{u=0}^1 \frac{1}{2} D^{i-uj-1} \langle \mathbf{c}^{i-uj-1} \rangle (F^{i-uj-1})^{-1} \\ T_{ij}^T &= \sum_{u=0}^1 \frac{1}{2} D^{i-uj} \langle \mathbf{c}^{i-uj} \rangle (F^{i-uj})^{-1}, \end{aligned} \quad (15)$$

and

$$\begin{aligned} q_{ij} &= \sum_{u,v=0}^1 [D^{i-uj-v} \langle \mathbf{c}^{i-uj-v} \rangle \\ &\quad + \frac{\mathbf{d}^{i-uj-v}}{2} \rangle (F^{i-uj-v})^{-1} (\bar{\phi}_{ij-v}^x + \bar{\phi}_{i-uj}^y) \\ &\quad + D^{i-uj-v} \langle \mathbf{d}^{i-uj-v} \rangle (F^{i-uj-v})^{-1} \\ &\quad \frac{1}{2} (\bar{\phi}_{i+1-2uj-v}^x + \bar{\phi}_{i-uj+1-2v}^y) \\ &\quad - D^{i-uj-v} \langle \mathbf{c}^{i-uj-v} + \mathbf{d}^{i-uj-v} \rangle \bar{\phi}_{i-uj-v}^x] \end{aligned} \quad (16)$$

In the above equations, \mathbf{c}^{ij} and \mathbf{d}^{ij} are diagonal matrices whose elements are given in Ref. 6.

The above equations (i.e., Eq.(8), Eq.(11), and Eq.(14) are solved by a conventional iteration method that consists of inner and outer iterations. At each inner iteration, the set of nodal coupling equations is solved sequentially by fixing the fission source and coupling coefficients to its values from the previous outer iteration. If the inner iteration converges, the multiplication factor and the fission source are updated by using the node average fluxes converged from the previous inner iteration. Also, the nodal coupling coefficients are updated by using the updated multiplication factor. Then a new inner iteration is performed. This procedure is continued until the relative errors of node average fluxes and multiplication factor satisfy the given criteria of convergence.

3. Adjoint Solutions of AFEN Method

3.1. Physical Adjoint

The starting equation is the continuous adjoint equation that is obtained by transposing the continuous diffusion equation (i.e., Eq.(1)). The equation is

given as follows:

$$- D^{*T} \nabla^2 \hat{\phi}^{*T}(x, y) + \Sigma^{*T} \hat{\phi}^{*T}(x, y) = \frac{1}{k_{eff}^p} \nu \Sigma_f^{*T} \hat{\phi}^{*T}(x, y) \quad (17)$$

where $\hat{\phi}^{*T}$ represents the physical adjoint flux, T denotes the transpose operation, and k_{eff}^p represents the eigenvalue of the physical adjoint equation.

This equation is discretized by the same procedure as in the forward equation in the AFEN formulation. Therefore, the nodal coupling equations of the physical adjoint equation have the same forms as those of the forward equation (Eq.(1)), while the coupling coefficients are very different from each other. So, the nodal coupling equations of the physical adjoint equation are solved by the same scheme as that of the forward equation. But the eigenvalues of the forward and physical adjoint equations are generally different from each other and the physical adjoint solution is mathematically not similar to the mathematical one. Also, the formulation of the physical adjoint equation is possible currently only for uncorrected nodal models (i.e., unit discontinuity factors) as mentioned in Introduction. Therefore, the physical adjoint cannot be generally used for perturbation theory.

Here, the physical adjoint flux and the eigenvalue are calculated so that these results are compared with those of the mathematical adjoint equation. In calculating the physical adjoint, the AFEN code is directly used, with minor modification.

3.2. Mathematical Adjoint

To derive the mathematical adjoint equation, the nodal coupling equations of the forward formulation (i.e., Eq.(8), Eq.(11), and Eq.(14)) are put into a single super-matrix form with matrices M and F , where M consists of the nodal coupling coefficient matrices and F the fission matrices:

$$M\Phi = \frac{1}{k_{eff}} F\Phi \quad (18)$$

where

$$\Phi = \text{col}([\bar{\phi}], [\bar{\phi}^x], [\bar{\phi}^y], [\bar{\phi}]),$$

$$M = \begin{bmatrix} [M_{00}] & [M_{0x}] & [M_{0y}] & [M_{0p}] \\ [M_{x0}] & [M_{xx}] & [M_{xy}] & [M_{xp}] \\ [M_{y0}] & [M_{yx}] & [M_{yy}] & [M_{yp}] \\ [M_{p0}] & [M_{px}] & [M_{py}] & [M_{pp}] \end{bmatrix}$$

and

$$F = \begin{bmatrix} [B] & [0] & [0] & [0] \\ [0] & [0] & [0] & [0] \\ [0] & [0] & [0] & [0] \\ [0] & [0] & [0] & [0] \end{bmatrix}$$

The mathematical adjoint equation is obtained by transposing Eq.(18). The equation is given as follows:

$$M^T \Phi^* = \frac{1}{k_{eff}} F^T \Phi^* \quad (19)$$

where Φ^* represents the mathematical adjoint flux vector.

This equation is solved by the same iterative schemes as those of the forward equation, in contrast to the mathematical adjoint of the QUANDRY code where the forward equation is solved first to calculate the eigenvalue to be used in solving the mathematical adjoint equation.

It must be noted that Eq.(19) was not directly derived from the continuous equation and its solution does not necessarily have obvious physical meanings. This solution is "mathematically" adjoint to that of Eq.(18). Since the matrices are transposed, the eigenvalue that is calculated from the mathematical adjoint equation should be the same as that of the forward equation.

4. Perturbation Theory for Reactivity

Since the perturbation theory provides the estimates of integral quantities without exact information for perturbed states, it has been widely used to estimate the effect of changes in nuclear systems.

The forward equation for an initial state is given by

Eq.(18) and the corresponding mathematical adjoint equation given by Eq.(19). To derive the perturbation expression for reactivity, now consider the introduction of a reactivity perturbation (e.g., material sample, control element, change in fuel temperature), which changes \mathbf{M} , \mathbf{F} , k_{eff} , and Ψ by $\delta\mathbf{M}$, $\delta\mathbf{F}$, δk_{eff} , and $\delta\Psi$ respectively, to

$$\begin{aligned}\widetilde{\mathbf{M}} &= \mathbf{M} + \delta\mathbf{M} \\ \widetilde{\mathbf{F}} &= \mathbf{F} + \delta\mathbf{F} \\ \widetilde{k}_{eff} &= k_{eff} + \delta k_{eff} \\ \widetilde{\Psi} &= \Psi + \delta\Psi.\end{aligned}\quad (20)$$

The forward equation for the perturbed state is given as follows:

$$\widetilde{\mathbf{M}}\widetilde{\Psi} = \frac{1}{\widetilde{k}_{eff}} \widetilde{\mathbf{F}}\widetilde{\Psi}.\quad (21)$$

To obtain an expression for the change in the criticality eigenvalue, first the perturbed forward equation (21) is premultiplied by the transposed mathematical adjoint flux:

$$\Psi^T \widetilde{\mathbf{M}} \widetilde{\Psi} = \frac{1}{\widetilde{k}_{eff}} \Psi^T \widetilde{\mathbf{F}} \widetilde{\Psi}.\quad (22)$$

Next the initial mathematical adjoint equation is premultiplied by transpose of the perturbed forward flux:

$$\widetilde{\Psi}^T \mathbf{M}^T \Psi = \frac{1}{k_{eff}} \widetilde{\Psi}^T \mathbf{F}^T \Psi.\quad (23)$$

Subtracting Eq.(23) from Eq.(22) and rearranging leads to an exact expression for the change in reactivity:

$$\delta\rho = \frac{\delta k_{eff}}{k_{eff} \widetilde{k}_{eff}} = - \frac{\Psi^T (\delta\mathbf{M} - \frac{1}{k_{eff}} \delta\mathbf{F}) \widetilde{\Psi}}{\Psi^T \widetilde{\mathbf{F}} \widetilde{\Psi}}.\quad (24)$$

In the above expression (24), the forward solution for the perturbed state is required but it cannot be obtained without solving the forward equation. Therefore, to estimate the effect of perturbation without

solving the perturbed state, an approximate expression is needed. For small perturbation, by inserting Eq.(20) into Eq.(24) and eliminating all second-order terms, a first-order perturbation formula for reactivity is obtained:

$$\delta\rho_0 = - \frac{\Psi^T (\delta\mathbf{M} - \frac{1}{k_{eff}} \delta\mathbf{F}) \Psi}{\Psi^T \mathbf{F} \Psi}.\quad (25)$$

It can be easily shown that the error in $\delta\rho_0$ is of first order with respect to $\delta\Psi$, i.e.,

$$\begin{aligned}\delta\rho - \delta\rho_0 &= \frac{\Psi^T (\delta\mathbf{M} - \frac{1}{k_{eff}} \delta\mathbf{F}) \delta\Psi}{\Psi^T \widetilde{\mathbf{F}} \widetilde{\Psi}} \\ &\quad - \frac{\Psi^T (\delta\mathbf{M} - \frac{1}{k_{eff}} \delta\mathbf{F}) \widetilde{\Psi}}{\Psi^T \widetilde{\mathbf{F}} \widetilde{\Psi}} - \frac{\Psi^T \widetilde{\mathbf{F}} \delta\Psi}{\Psi^T \widetilde{\mathbf{F}} \widetilde{\Psi}} \\ &\quad + O(\delta\Psi^T \delta\Psi).\end{aligned}\quad (26)$$

Therefore, the formula Eq.(25) provides the first-order estimate of the reactivity change.

5. Application and Results

To verify the adjoint solution that is calculated in the AFEN method, two benchmark problems were selected. The first is the International Atomic Energy Agency (IAEA) two-dimensional (2D) benchmark problem where the core consists of fully homogenized fuel assemblies. The configuration of this benchmark problem is shown in Fig. 1 and the macroscopic cross sections are given in Table 1. The second is the Electric Power Research Institute (EPRI) 9R benchmark problem where the core consists of heterogeneous assemblies with different types of 15×15 homogenized pin cells. This benchmark problem was selected for consideration of the nodal model with discontinuity factors not equal to unity. There are two configurations in the EPRI-9R benchmark problem: one is unrodded, and the other is rodded at the core center assembly. Here, the latter was solved. The configuration of the EPRI-9R benchmark

problem is shown in Fig. 2 and the homogenized macroscopic cross sections are given in Table 2. The discontinuity factors for surfaces and corner points are given in Table 3.

Our strategy that calculates the change of reactivity by perturbation theory given in Section 4 consists of two steps. The first step is to calculate the adjoints (physical adjoint or mathematical adjoint) by solving

Table 1. Macroscopic Cross Sections(cm^{-1}) of the Homogenized Assemblies for the IAEA-2D Benchmark Problem*

Assembly type	group	D	Σ_a	$\Sigma_{1 \rightarrow 2}$	$\nu\Sigma_f$
type 1	fast	1.500	0.010	0.020	0.000
	thermal	0.400	0.080		0.135
type 2	fast	1.500	0.010	0.020	0.000
	thermal	0.400	0.085		0.135
type 3	fast	1.500	0.010	0.020	0.000
	thermal	0.400	0.013		0.135
type 4	fast	2.000	0.000	0.040	0.000
	thermal	0.300	0.010		0.000

* Fast group axial buckling: 8.0×10^{-5} , Thermal group axial buckling: 8.0×10^{-5}

Table 2. Macroscopic Cross Sections(cm^{-1}) of the Homogenized Assemblies for the EPRI-9R Benchmark Problem

Assembly type	group	D	Σ_a	$\Sigma_{1 \rightarrow 2}$	$\nu\Sigma_f$
type 1	fast	1.5133400	0.0121010	0.0211238	0.0060130
	thermal	0.3948540	0.1681400		0.2181040
type 2	fast	1.5133300	0.0093259	0.0211340	0.0046255
	thermal	0.3950120	0.1411600		0.1640890
type 3	fast	1.4657600	0.0147702	0.0189548	0.0046336
	thermal	0.3850950	0.1754670		0.1729620
type 4	fast	1.3509500	0.0018526	0.0214356	0.000000
	thermal	0.3482930	0.0605073		0.000000

Table 3. Discontinuity Factors for the EPRI-9R Benchmark Problem

Assembly type	group	SDF	PDF
type 1 (F-1(W))	fast	1.003040	1.003753
	thermal	0.928806	0.912237
type 2 (F-2(W))	fast	1.003640	1.004826
	thermal	0.938578	0.922818
type 3 (F-2(CR))	fast	1.016150	1.029787
	thermal	1.139440	1.189693
type 4 (Reflector)	fast	1.159790	1.159790
	thermal	0.289747	0.289747

the adjoint equations. In the case of physical adjoint, the adjoint is obtained by using the AFEN code with minor modification, but for the mathematical adjoint a new program was written through a modification of the AFEN code. The second step is to estimate the change of reactivity by the perturbation formulas with the results of the first step. Here, exact and first-order

perturbation calculations were performed for comparison of the results.

For IAEA-2D benchmark problem, the physical adjoint, mathematical adjoint, and their eigenvalues were calculated within convergence criteria of 10^{-8} for both eigenvalue and node average flux. These results were compared with those of the VENTURE code. The fine mesh calculation of VENTURE, which uses the mesh-centered finite difference method, is used as reference values. These results are given in Table 4.

To estimate the change of reactivity by the perturbation theory, the macroscopic absorption cross sections of type 2 assemblies are changed from $0.085(\text{cm}^{-1})$ to $0.086(\text{cm}^{-1})$. This perturbation is a relatively global change rather than a local one, since the type 2 assemblies are distributed widely over the core. The results of the perturbation calculation are given in Table 5. The exact and first-order perturbation calculations were performed to estimate the change of the reactivity. As expected, the forward and mathematical adjoint eigenvalues were equivalent to each other but these were slightly different from the physical adjoint eigenvalue. This equivalence demonstrates that our mathematical adjoint flux is the correct solution of the mathematical adjoint equation of the AFEN method. Further, the result of the exact per-

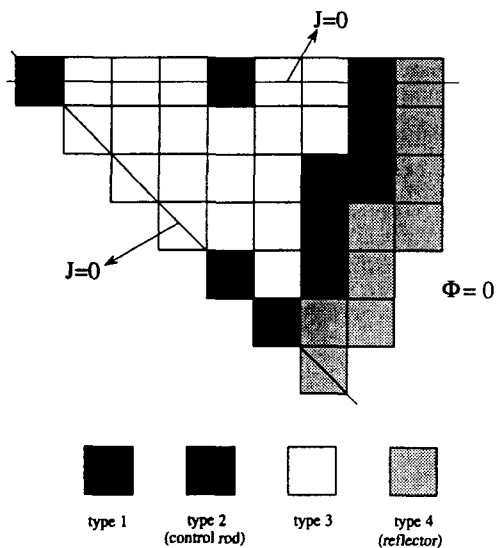


Fig. 1. Configuration of the IAEA-2D Benchmark Problem

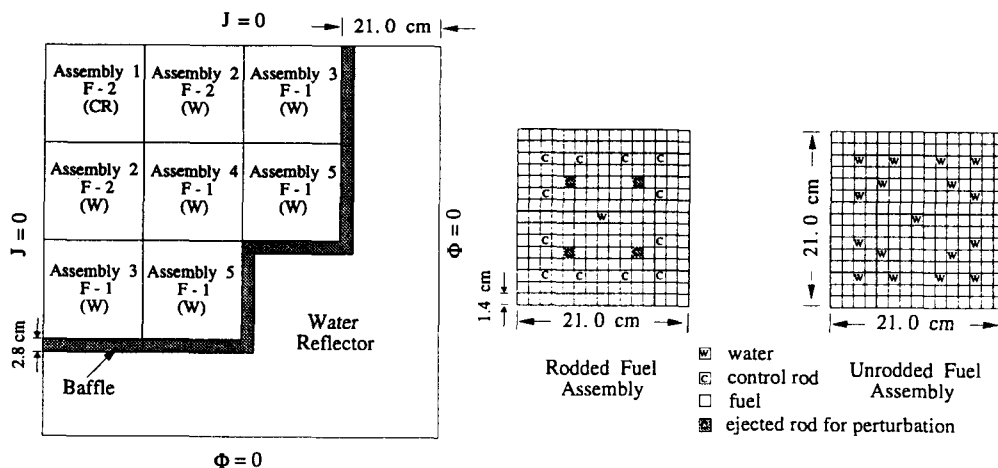


Fig. 2. Configuration of the EPRI-9R Benchmark Problem

turbation calculation exactly coincided with that of the direct forward calculation by solving the perturbed state. Also, it is noted that the first-order perturbation calculation provides a quite accurate estimate of the reactivity change.

To consider the nodal model with discontinuity factors not equal to unity, the adjoint option in the AFEN code was applied to the EPRI-9R benchmark problem. First to verify the result of the mathematical adjoint flux in the AFEN code, the eigenvalues were calculated by the VENTURE code, the AFEN code (forward option), and the adjoint option in the AFEN code solving the mathematical adjoint equation. The results are given in Table 6. Table 6 shows that the forward and mathematical adjoint eigenvalues were equivalent to each other as before. But the physical adjoint of the AFEN method has not been defined. To estimate the reactivity change, the initial state is

perturbed by withdrawing four control rods (marked as shaded rods in Fig. 2) in the most central assembly. This perturbation results in a change of the homogenized assembly cross sections and the discontinuity factors. These perturbed data are given in Table 7. The results of perturbation calculations are given in Table 8. As in the IAEA-2D benchmark problem, the forward and mathematical adjoint eigenvalues were equivalent to each other and this result demonstrates that our mathematical adjoint flux is the correct solution of the adjoint equation in AFEN with discontinuity factors. But, it is noted that the first-order perturbation calculation provides more or less a poor estimate of the reactivity for this benchmark problem of which core size is quite small.

As a note, there may exist many different mathematical adjoint solutions for a given forward solution but these adjoint solutions are not independent

Table 4. Comparison of Eigenvalues for the IAEA-2D Benchmark Problem

Methods	Eigenvalues	Relative error(%) to VENTURE
Forward	1.029570	0.0017
Physical adjoint	1.029370	0.0014
Mathematical adjoint	1.029570	0.0017
VENTURE	1.029552	ref.

** Mesh size in VENTURE: 0.625cm

** Mesh size in AFEN: 20cm (assembly size)

Table 6. Comparison of Eigenvalues for the EPRI-9R Benchmark Problem

Methods	Eigenvalues	Relative error(%) to VENTURE
Forward	0.8891072	0.12
Mathematical adjoint	0.8891072	0.12
VENTURE	0.8901810	ref.

** Mesh size in VENTURE: 0.7cm (2x2meshes/pincell)

** Mesh size in AFEN: 21cm (assembly size)

Table 5. Results of Perturbation Calculations for the IAEA-2D Benchmark Problem

Methods	Perturbed eigenvalues	Reactivity changes
Forward	1.019874(a)	-0.009234
Mathematical adjoint	1.019874(a)	-0.009234
VENTURE	1.019845(a)	-0.009245
First-order perturbation theory	1.019668(b)	-0.009432
Exact perturbation theory	1.019874(c)	-0.009234

(a) obtained by solving the perturbed state

(b) obtained by Eq.(25)

(c) obtained by Eq.(24)

Table 7. Perturbed Homogenized Cross Sections and Discontinuity Factors

group	D	Σ_a	$\Sigma_{1 \rightarrow 2}$	$\nu \Sigma_f$	SDF	PDF
fast	1.48393E+00	1.37262E-02	1.94802E-02	4.61796E-03	1.03623E+00	1.04195E+00
thermal	3.93053E-01	1.67338E-01		1.70009E-01	1.08405E+00	1.11826E+00

Table 8. Results of Perturbation Calculation for the EPRI-9R Benchmark Problem

Methods	Perturbed eigenvalues	Reactivity changes
Forward	0.8929865	0.004886
Mathematical adjoint	0.8929865	0.004886
VENTURE	0.8943962	0.005294
First-order perturbation theory	0.8967582	0.009596
Exact perturbation theory	0.8929865	0.004886

of each other, that is to say, these adjoint solutions are related with simple linear transformations. Therefore, all these mathematical adjoints are equivalent and can be used in perturbation calculation with their consistent perturbation formula.

6. Conclusions

Since it is well-known that the forward solution of the AFEN method is highly accurate in most problems, the corresponding adjoint solution if available will be very useful to estimate the effects of changes in a reactor by perturbation theory.

In this work, the mathematical adjoint flux of the AFEN method was found for application to many reactor analysis problems. The mathematical adjoint solution is calculated directly by the forward solution scheme with minor modification in the AFEN code. The calculational scheme does not require the knowledge of the physical adjoint (physical adjoint itself cannot be defined well for realistic problems) or the eigenvalue of the forward equation, unlike some existing methods. The adjoint flux thus obtained was used to estimate the reactivity change by the exact and first-order perturbation theory. The results show that our mathematical adjoint flux is the correct adjoint solution of the AFEN method.

Acknowledgment

The authors are indebted to Jae Man Noh for helpful discussions during the course of this work.

References

1. T.A. TAIWO, A.F. HENRY, "Perturbation Theory Based on a Nodal Model," *Nuclear Science and Engineering*, **92**, 34 (1986).
2. R.D. LAWRENCE, "Perturbation Theory Within the Framework of a Higher Order Nodal Method," *Trans. Am. Nucl. Soc.*, **46**, 402 (1984).
3. T.A. TAIWO, "Mathematical Adjoint Solution to the Nodal Code QUANDRY," *Trans. Am. Nucl. Soc.*, **55**, 580 (1987).
4. W.S. YANG, T.A. TAIWO, and H. KHALIL, "Solution of the Mathematical Adjoint Equations for an Interface Current Nodal Formulation," *Nuclear Science and Engineering*, **116**, 42 (1994).
5. W.S. YANG, "Similarity Transformation Procedure for Nodal Adjoint Calculations," *Trans. Am. Nucl. Soc.*, **66**, 270 (1992).
6. J.M. Noh, N.Z. Cho, "A New Approach of Analytic Basis Function Expansion to Neutron Diffusion Nodal Calculation," *Nuclear Science and Engineering*, **116**, 165 (1994).

7. J.M. Noh, N.Z. Cho, "Analytic Function Expansion Nodal Method for Hexagonal Nodes," *Proc. 1994 Topl. Mtg. on Advances in Reactor Physics*, Knoxville, Tennessee, April 11–15, 1994, Vol. I, p. 95, American Nuclear Society (1994).
8. N.Z. Cho, J.M. Noh, "The AFEN Method for Hexagonal Nodal Calculation and Reconstruction," *Trans. Am. Nucl. Soc.*, **71**, 466 (1994).
9. N.Z. Cho, J.M. Noh, "Analytic Function Expansion Nodal Method for Hexagonal Geometry," *Nuclear Science and Engineering*, accepted, October 1994.
10. N.Z. Cho, D.S. Kim, "On the AFEN Method for Triangular Nodes in Hexagonal Assembly Cores," *Proc. of Korean Nucl. Soc. Spring Meeting*, Ulsan, Korea, May 1995.